

# First Demonstration of a Combined Light and Charge Pixel Readout on the Anode Plane of a LArTPC

---

## SoLAr Collaboration

N. Anfimov,<sup>13</sup> A. Branca,<sup>6,10</sup> J. Bürgi,<sup>1</sup> L. Calivers,<sup>1</sup> C. Cuesta,<sup>3</sup> R. Diurba,<sup>1</sup> P. Dunne,<sup>5</sup> D. A. Dwyer,<sup>7</sup> J. J. Evans,<sup>9</sup> A. C. Ezeribe,<sup>12</sup> A. Gauch,<sup>1</sup> I. Gil-Botella,<sup>3</sup> S. Greenberg,<sup>2,7</sup> D. Guffanti,<sup>6,10</sup> A. Karcher,<sup>7</sup> I. Kreslo,<sup>1</sup> J. Kunzmann,<sup>1</sup> N. Lane,<sup>9</sup> S. Manthey Corchado,<sup>3</sup> N. McConkey,<sup>11</sup> A. Navrer-Agasson,<sup>5,9</sup> S. Parsa,<sup>1</sup> G. Ruiz Ferreira,<sup>9</sup> B. Russell,<sup>8</sup> A. Selyunin,<sup>13</sup> S. Söldner-Rembold,<sup>5,9</sup> A. M. Szec,<sup>4</sup> A. Tapper,<sup>5</sup> F. Terranova,<sup>6,10</sup> C. Tognina,<sup>1</sup> G. V. Stenico,<sup>4</sup> M. Weber,<sup>1</sup> and I. Xiotidis<sup>5</sup>

<sup>1</sup>University of Bern, CH-3012 Bern, Switzerland

<sup>2</sup>University of California Berkeley, Berkeley, CA 94720, USA

<sup>3</sup>CIEMAT, Centro de Investigaciones Energéticas, Medioambientales y Tecnológicas, E-28040 Madrid, Spain

<sup>4</sup>University of Edinburgh, Edinburgh EH9 3FD, United Kingdom

<sup>5</sup>Imperial College of Science, Technology and Medicine, London SW7 2BZ, United Kingdom

<sup>6</sup>Istituto Nazionale di Fisica Nucleare Sezione di Milano Bicocca, 3 - I-20126 Milano, Italy

<sup>7</sup>Lawrence Berkeley National Laboratory, Berkeley, CA 94720, USA

<sup>8</sup>Massachusetts Institute of Technology, Massachusetts, MA 02139, USA

<sup>9</sup>University of Manchester, Manchester M13 9PL, United Kingdom

<sup>10</sup>Università di Milano-Bicocca, I-20126 Milano, Italy

<sup>11</sup>Queen Mary University of London, London E1 4NS, United Kingdom

<sup>12</sup>University of Sheffield, Sheffield S3 7RH, United Kingdom

<sup>13</sup>Visitor

E-mail: [saba.parsa@cern.ch](mailto:saba.parsa@cern.ch)

**ABSTRACT:** The novel SoLAr concept aims to extend sensitivities of liquid-argon neutrino detectors down to the MeV scale for next-generation detectors. SoLAr plans to accomplish this with a liquid-argon time projection chamber that employs an anode plane with dual charge and light readout, which enables precision matching of light and charge signals for data acquisition and reconstruction purposes. We present the results of a first demonstration of the SoLAr detector concept with a small-scale prototype detector integrating a pixel-based charge readout and silicon photomultipliers on a shared printed circuit board. We discuss the design of the prototype, and its operation and performance, highlighting the capability of such a detector design.

**KEYWORDS:** Noble liquid detectors (scintillation, ionization, single-phase), time projection chambers, neutrino detectors

---

## Contents

<b>1</b>	<b>Introduction</b>	<b>1</b>
<b>2</b>	<b>Experimental Setup</b>	<b>2</b>
2.1	Design of the SoLAr prototype Time Projection Chamber	2
2.2	Electric field simulation	5
2.3	Cryogenics system	5
<b>3</b>	<b>Results</b>	<b>6</b>
3.1	Prototype Operation	6
3.2	First cosmic-ray tracks with dual-pixel light and charge readout	7
3.3	Charge collection per unit length	8
3.4	Light collection as a function of SiPM floating voltages	9
<b>4</b>	<b>Summary</b>	<b>10</b>

---

## 1 Introduction

The next generation of deep underground detectors, DUNE [1] and Hyper-Kamiokande [2], will enable a substantial leap in the sensitivity of neutrino physics experiment through their detectors' mass and precision. Their baseline design is optimized for the detection of GeV-scale neutrinos produced by a particle beam with the goal to measure oscillation parameters with unprecedented precision [3]. In addition, the large mass and the underground location of the detectors provide a unique opportunity to expand their sensitivity to lower energy neutrinos, with energies at the MeV-scale, originating from natural nuclear processes.

Solar neutrinos provide an avenue for these future detectors to explore, primarily to detect neutrinos generated from the *hep* branch [4, 5]. Its discovery directly impacts the modeling of our Sun and the modeling of stellar evolution throughout the Universe. The application of liquid-argon detectors to solar-neutrino physics has been explored previously [6–8]. Such a detector was found to need an energy resolution at the MeV-scale of 7% to measure solar neutrinos [6], to have excellent background rejection capabilities, and to have reasonably low data rates. These requirements are essential to successfully discriminate the higher-energy tail of the *hep* neutrino spectrum from the dominant  ${}^8\text{B}$  neutrino spectrum.

One significant challenge is related to readout and computing. The whole DUNE Far Detector site needs to collect petabytes of light and charge data per year to accomplish its calibration and neutrino programs from natural sources [1]. Providing a solution that enables large mass detectors while limiting data rates would significantly increase the feasibility of low-energy searches in liquid-argon detectors.

Supernova explosions eject most of their energy in form of neutrinos with energies similar to those of *hep* neutrinos. A detector that is able to observe *hep* neutrinos is by construction also the most precise experiment to detect supernova explosions. Combining the data with visible, X-ray,  $\gamma$ -ray, and gravitational-wave information will provide a complete picture of the supernova collapse [9].

The SoLAr collaboration proposes to build multipurpose liquid-argon time projection chambers (LArTPCs) with several kilotons of active mass to detect beam neutrinos, supernova neutrinos, solar neutrinos, and to search for *hep* neutrinos [10]. The main feature of the SoLAr proposal consists of a pixel-based dual-readout anode plane combining charge and light readout to increase energy resolution, improve background rejection, and decrease data storage requirements.

The pixel-based charge readout accomplishes these goals through native three-dimensional reconstruction. The proposal builds on the progress of pixel-based LArTPCs being constructed for the Near Detector site at DUNE [11]. In this detector, light-readout systems will be mounted either underneath or directly next to the pixels on the anode plane, providing two-dimensional light reconstruction to accompany the signals from the neighboring charge pixels.

The development of silicon photomultipliers (SiPMs) sensitive to vacuum ultraviolet (VUV) light is instrumental to the SoLAr proposal. The combination with charge readout allows for greater sensitivities in reconstruction through light and charge signal matching. It opens possibilities in online triggering by sectorizing the detector and triggering specific pixels only when its neighboring light detector sees a signal.

We aim to use the design concept to build an  $\approx 10$  t liquid-argon SoLAr-type detector with an active volume of about  $1.6 \times 2 \times 2.6$  m<sup>3</sup>. Early planning has found the Boulby Underground Laboratory in the United Kingdom as a suitable location. The Boulby Laboratory is located in a working polyhalite and salt mine in the North East of England at a depth of 1.1 km. The SoLAr detector concept could also be adapted for the instrumentation of future Far Detector modules for DUNE [10] as part of the DUNE Phase-II programme [12, 13].

In this paper, we describe the design of the first SoLAr prototype TPC and present results from the operation of this prototype at the University of Bern in October 2022.

## 2 Experimental Setup

### 2.1 Design of the SoLAr prototype Time Projection Chamber

The first SoLAr prototype TPC (Prototype-v1) uses a printed circuit board (PCB) with a pixelated charge readout system using the LArPix chip [14] and neighboring Hamamatsu VUV SiPMs. The PCB acts as the anode plane and is placed within an electric field to measure the ionization charge in the liquid argon. The liquid argon VUV scintillation light from cosmic-ray muons is measured by the SiPMs. The dimensions of the TPC are  $11.8 \times 10.8$  cm<sup>2</sup> in the  $x$  and  $y$  direction, with a sensitive anode area of  $7 \times 7$  cm<sup>2</sup>, and 5 cm in the drift direction ( $z$ ). The choice is driven by the cryostat inner volume geometry, which has a diameter of 14 cm. This size is sufficient to demonstrate the SoLAr concept by collecting light and charge from cosmic rays on the same plane.

The active area of the LArTPC is divided into a grid of 16 identical cells. Each cell consists of a VUV SiPM (Hamamatsu S13370-6050CN) and 16 charge-collection pads, resulting in a total

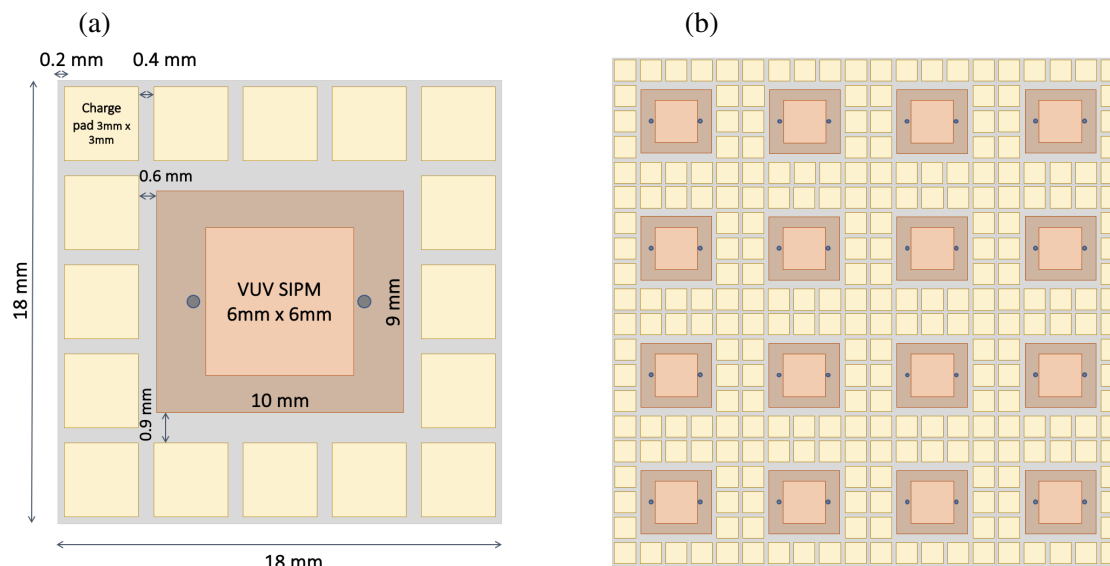


**Figure 1.** (a) Schematic of a single cell within the sensitive area of the LArTPC. Charge-collecting pixels are located directly next to the pin of each SiPM; (b) the complete v1 prototype with all 16 cells.

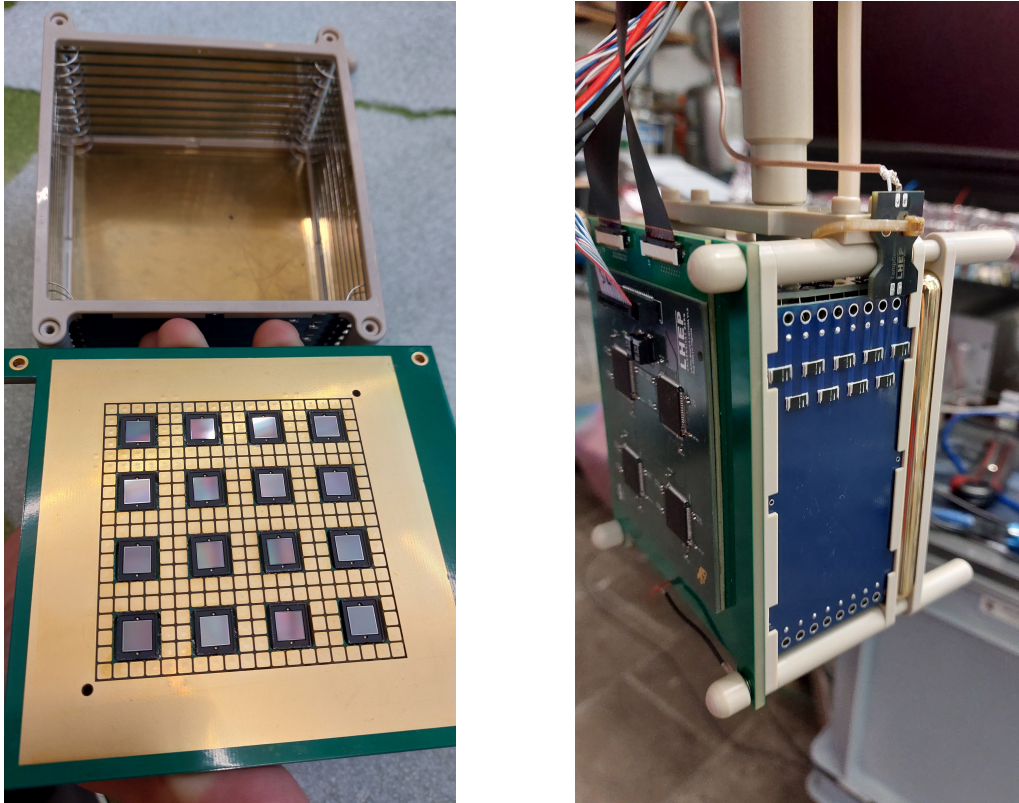
of 256 pixels (see Figure 1). The cathode is a 1 cm thick metal plate with smooth golden surface and rounded corners to prevent discharges to the cryostat walls for potentials up to 10 kV. The side panel PCBs on the four walls function as electric field shaping surfaces with nine metalized bands linked through a resistor chain to create a homogeneous electric field along the electrons' drift line from the cathode to the anode.

Figure 2 shows the interior of the TPC with the cathode plate, side panel PCBs, and the readout anode plate. The assembled TPC connected to a hanging fixture is shown in Figure 2. The rounded corner rods extending out of the TPC volume are mechanical guides for insertion into the cryostat and for adjusting the position and distances of the TPC from the cryostat's inner walls.

The VUV SiPMs collect the photons in Geiger mode and transfer the analog light waveform signal to a cold pre-amplifier stage over a short (20 cm) double-layered flex PCB. The signal is then transferred via a feed-through PCB using SAMTEC micro-coaxial cables to a variable gain amplification (VGA) unit. The differential amplified signal at this stage is transferred via a twisted-pair ribbon cable to an analog-to-digital converter (ADC) unit.

The charge collected on the pixel pads is read out with the help of a LArPix chip, a cryo-rated ASIC for pixelated liquid-argon TPCs, developed by LBNL [14]. Four LArPix chips are used to read out the 256 pixels on the anode plane. The LArPix chip provides a self-triggering digitization and multiplexed data transfer to a readout hub in warm, referred to as the PACMAN. The anode readout plane consists of three layers of PCBs mounted on top of each other, as shown in Figure 3. The charge collection pads are located on the innermost layer, which contains cutout holes to accommodate the SiPMs soldered on the second layer. This configuration ensures that the surfaces of the ceramic-packaged SiPMs are level with the charge collection pixels. This alignment minimizes electric field deformations near the edges of the SiPMs and charge collection pads. The second layer hosts the SiPMs and their readout traces to the connectors. It also contains a network

of traces that transmits the charge signals to the outermost layer, which hosts the LArPix readout chips and charge readout connector.



**Figure 2.** (left) Interior of the SoLAR-v1 TPC time projection chamber with the cathode plate, the side panels for  $E$ -field shaping and the readout anode plate containing the SiPMs and charge pixels. (right) Fully assembled SoLAR-v1 TPC attached to its support structure. The back side of the anode plate with the four LArPix chips and the back side of one of the  $E$ -field shaping panels with a resistor chain is also visible.

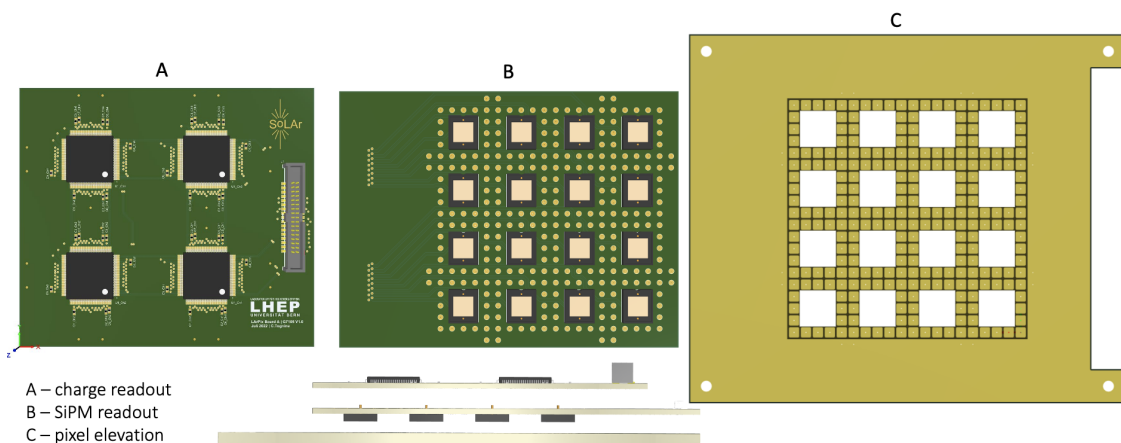


**Figure 3.** Top and side-view of the anode readout plane three-layer stack: charge (A) and SiPM readout (B), and pixel elevation (C).

The SiPMs operate at a bias voltage of 56 V at room temperature and 46 V at liquid-argon temperature. The setup is designed to provide floating bias voltages on the SiPMs, such that the top surface of the SiPMs facing the TPC interior could be set to a negative floating voltage compared to the ground of the charge pads. In this way, the potential on the SiPMs surface can shape the electric fields toward the pixels, potentially increasing the charge collection efficiency.

## 2.2 Electric field simulation

To understand the impact of design choices on the charge collection, the electric field in proximity of the anode was evaluated numerically using the COMSOL package [15]. Figure 4 shows the results for the electric field lines.

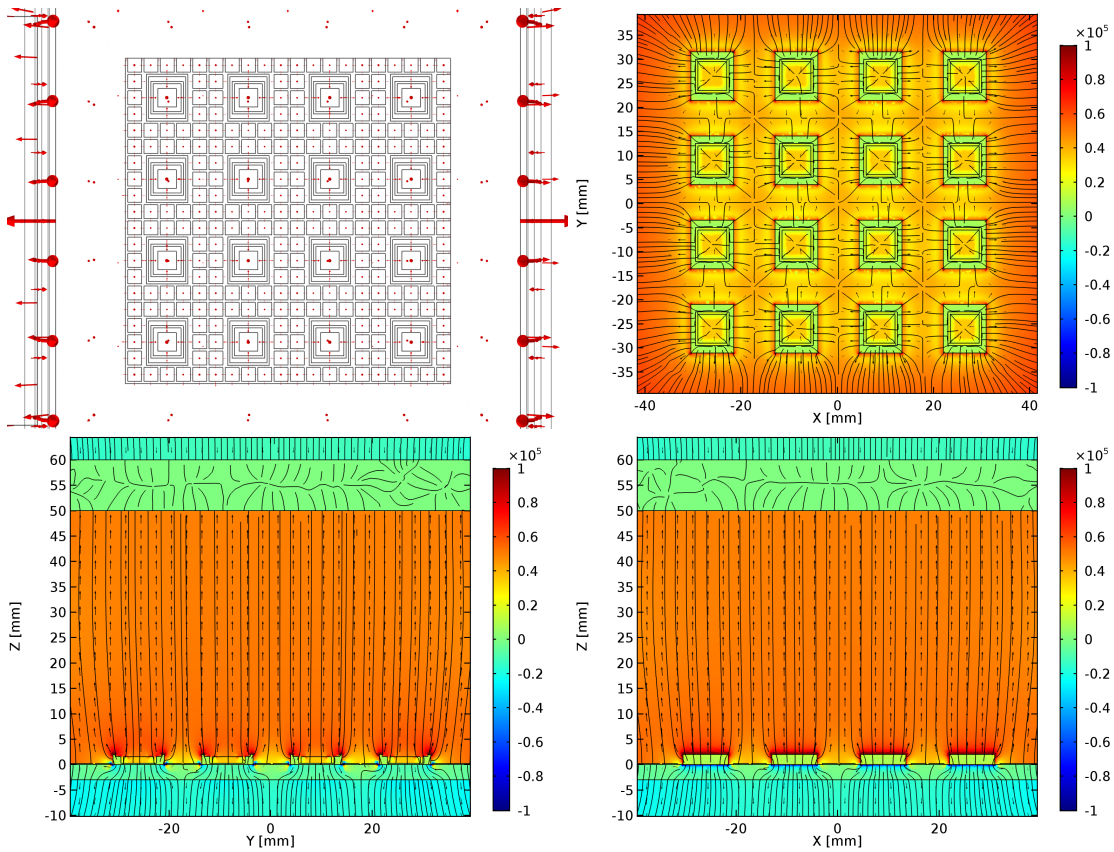


**Figure 4.** (Top) COMSOL numerical evaluation showing the direction and magnitude of the electric field on the anode plane ( $x, y$ ). The SiPM surface potential is set to ground. (Bottom) COMSOL electric field numerical evaluation showing the field lines in the drift direction  $z$ .

## 2.3 Cryogenics system

We used a triple-layer cryostat to operate the SoLAr prototype with liquid argon. A vacuum jacket provides thermal insulation for the two volumes of the cryostat. The outer volume is used as a cooling jacket with liquid argon constantly flowing through this layer. The inner volume of the cryostat is filled with liquid argon once and sealed for the full duration of the run. Figure 5 shows a schematic of the SoLAr Prototype-v1 in the cryostat.

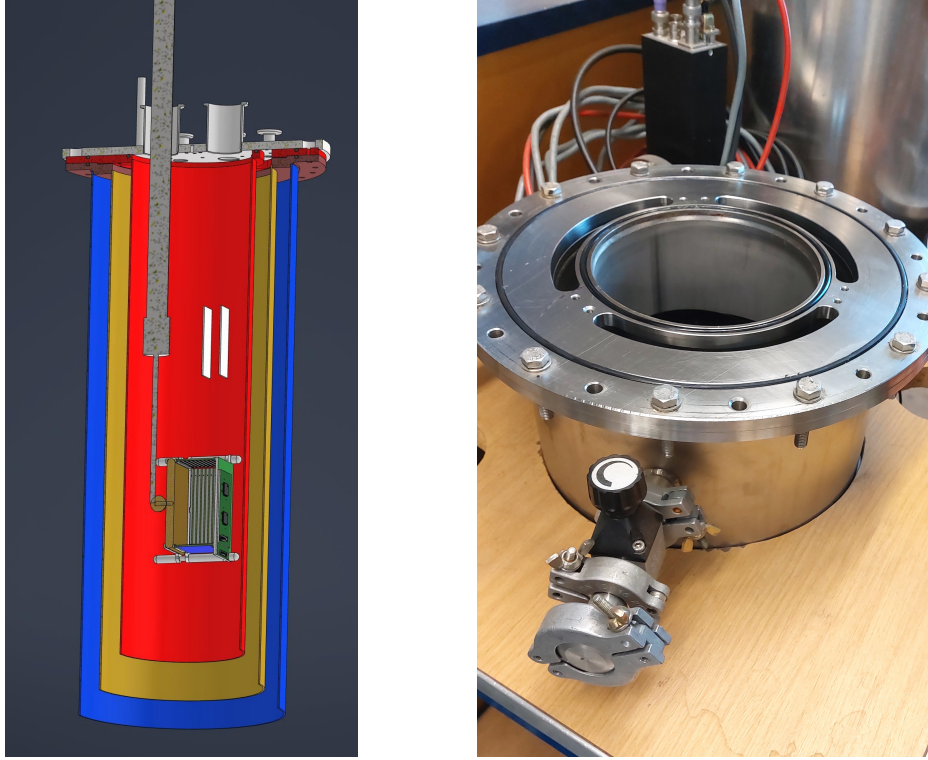


**Figure 5.** (a) Section view of the CAD drawing of the cryostat and the SoLAR prototype. The blue region is indicating the vacuum jacket, the orange region is the outer volume, and the red region is the inner volume with the prototype detector inside. (b) The cryostat with open lid, where the access to separate volumes is visible.

The liquid argon passes through a filling filter with copper getters to remove traces of oxygen and humidity from the LAr. This small setup is not equipped with re-circulation capabilities and thus the purity of the LAr will deteriorate over time, giving us a short window to bring up the system and take cosmic-ray data.

The level of liquid argon inside the cryostat is controlled with three temperature sensors at different heights connected to the slow control system. The slow control system and each readout system has an individual feed through on the cryostat to transfer data. The bias voltage for the SiPMs is routed through a separate feed through in order to allow different schemes of floating from ground. The pressure in the layers of the cryostat is monitored with two pressure gauges, mounted on the top flange. The inner volume is kept at an overpressure of 50 mbar for the duration of the test. Figure 6 shows the top flange with the assembled SoLAR Prototype-v1 TPC shortly before insertion into the cryostat and the experimental setup during cryogenic operation.

### 3 Results

#### 3.1 Prototype Operation

In this section, we describe the results obtained with the light and charge readout based on data collected during the cryogenics operation at the University of Bern during October 24–26, 2022.

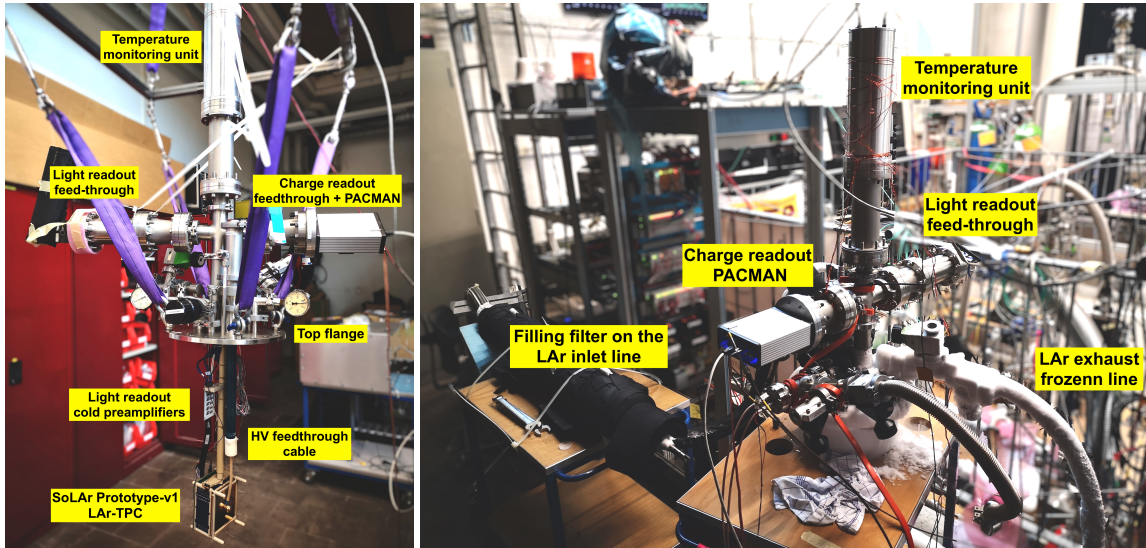


**Figure 6.** (a) Top flange with all the feed-throughs and the suspended SoLAr Prototype-v1 LArTPC shortly before inserting it into the cryostat. (b) Experimental setup during cryogenics operation.

After the cryostat had been filled with liquid argon and the temperature sensors had been submerged, the cathode voltage was raised to a potential of 2.5 kV to provide an electric field of 500 V/cm.

The data was collected for both the charge and the light readout continuously with separate self-triggering data acquisition systems. In order to synchronize, a pulse per second signal from the Global Positioning System (GPS) was fed to both systems. In addition, a light trigger signal was sent to the charge readout PACMAN, which is written into the charge data stream as a  $t_0$  marker to identify the start time of an event. This enables correct association of the charge packets' drift time.

The charge and light data have universal time stamps associated with the signals measured on both readout systems. These time stamps are used in offline data processing to associate the light and charge signals, creating what we defined as “events”, with each event covering a time span of 200  $\mu$ s. The drift distance of 5 cm requires  $\approx 60 \mu$ s for an electron to travel the full drift length. The event window is therefore long enough so that all the charge that is created through ionization at the time  $t_0$  can drift from the cathode to the anode. If two light signals occur in close proximity, only the earliest light signal is used to mark the start of an event. This can potentially cause some event mismatching which has to be taken into account in the analysis.

### 3.2 First cosmic-ray tracks with dual-pixel light and charge readout

In Figure 7, we show two representative events, out of around 70,000 collected during the October 2022 run. The  $x$  and  $y$  axes represent the span of the anode plane, while the  $z$  direction indicates the drift distance between the anode and the cathode. The patterns of charge and light signals on the pixels clearly indicate a muon track candidate. The  $zy$  projection is obtained by extrapolating the drift distance of the electrons to the anode plane using the light trigger time  $t_0$ . They provide an unambiguous three-dimensional hit object. This result represents the first combined detection of charge and light on a dual-pixel anode plane in a LArTPC, which is a major milestone for



demonstrating the fully three-dimensional charge and light association of the SoLAr concept for triggering and reconstruction purposes [10].

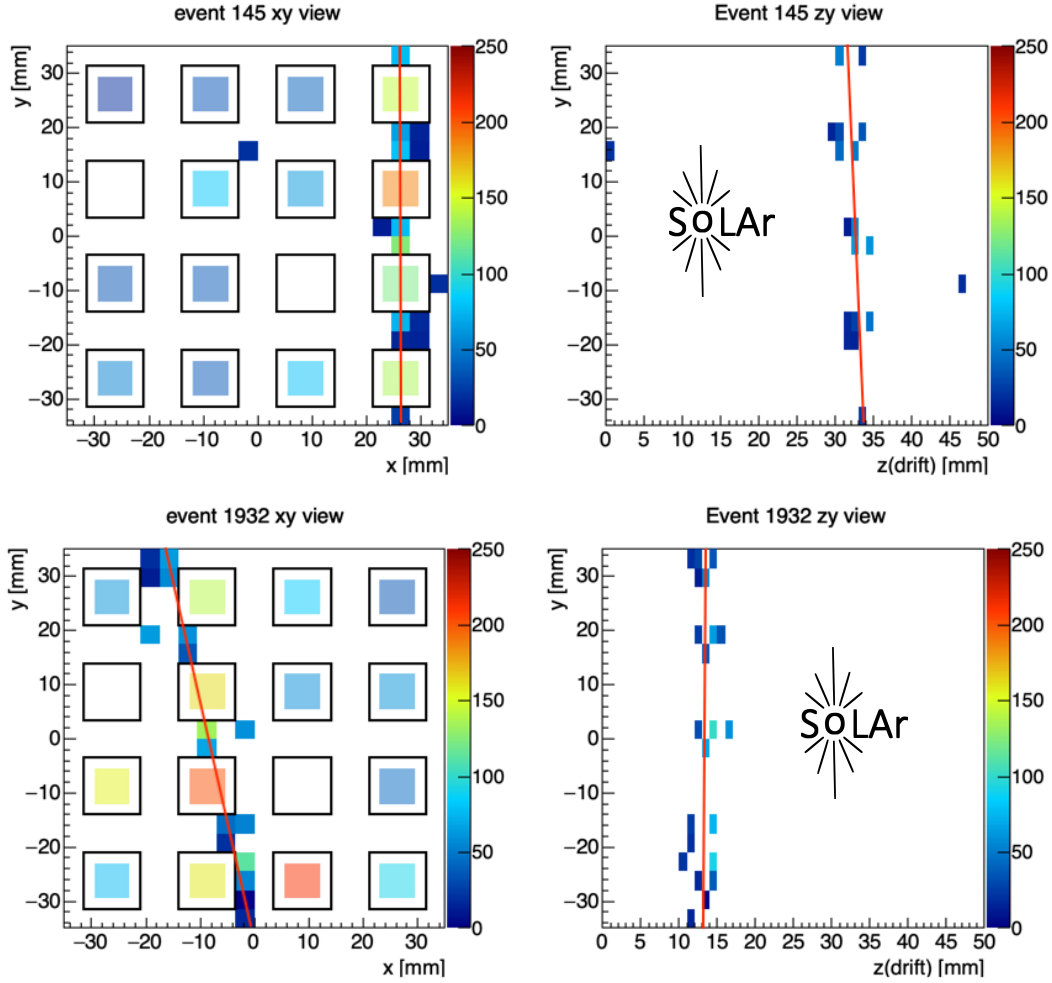


**Figure 7.** Two cosmic-ray events recorded by the prototype shown from the anode view in the  $xy$  plane and as  $zy$  view, where  $z$  is the drift direction. The  $xy$  views show the total light detected by each SiPM in the larger square pads and the amount of collected charge on each pixel in the smaller square pads. The color scale represents relative intensity in ADC units. Its range is tuned for visual aid.

### 3.3 Charge collection per unit length

We evaluate the amount of charge per unit length ( $dQ/dx$ ) on selected events using through-going tracks selected by applying linear fits to the charge data. These tracks are analyzed pixel-by-pixel to measure the total amount of charge each pixel records from what is likely a minimally ionizing cosmic-ray muon. Figure 8 shows the distribution of charge per unit length for through-going tracks over a data-taking period of 10 minutes for 0 V floating scheme. The value of each individual pixel channel is subtracted by the value of said channel from a previously taken pedestal run to equalize the baseline of said channels. Because approximately half of the pixels were not functional, the

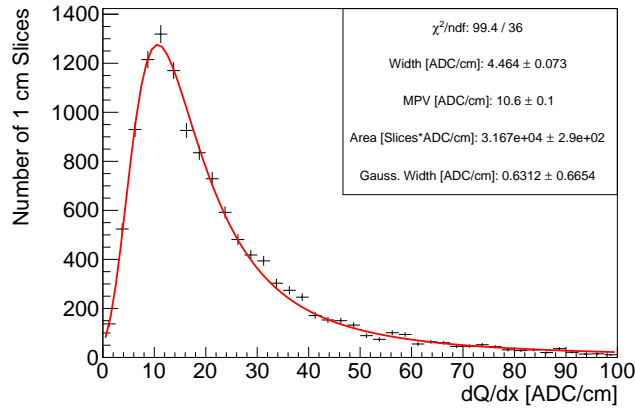


**Figure 8.** Charge deposit per unit length for through going cosmic-ray particles. The uncertainties on the data points are statistical. Each slice has a length of 1 cm.

purpose of this study is to show that calorimetry with the charge information can be represented by a Landau-Gaussian function. The measurements are presented in ADC/cm.

As expected, the distribution of electrons per unit length follows a Landau-Gaussian distribution, which is consistent with the result of a fit [16]. The result suggests that the SoLAR Prototype-v1 charge readout system can carry out basic charge-based calorimetry. Further calibration and larger-scale prototypes are necessary to obtain results comparable to similar pixelated prototype detectors [17] since the volume of the field shell and the active detector area for charge collection are small, leading to charge loss.

### 3.4 Light collection as a function of SiPM floating voltages

The setup is designed with the possibility to float the voltage level of the SiPMs with respect to the ground level on the anode surface and the charge collection pads. In this scheme, the voltage level of both pins of the SiPMs is simultaneously shifted by a fixed amount while the SiPM bias, the difference between potential of the two SiPM pins, is kept at the same value of 46 V.

Floating the SiPMs to a negative potential may increase the effective charge collection of neighboring pads by deforming the electric field lines and thus diverting the drifting electrons away from the SiPMs surface and to the charge collection pixels (see Figure 4). We study the amount of collected light as a function of the floating voltage applied to the SiPMs by comparing the average number of detected photons per unit length of through-going muon tracks for different floating voltage levels.

Figure 9 shows the number of photo-electrons collected for each floating level relative to the mean number of collected photo-electrons without any floating voltage applied to the SiPMs. As expected, the signal strength as a function of floating voltages is constant within uncertainties.

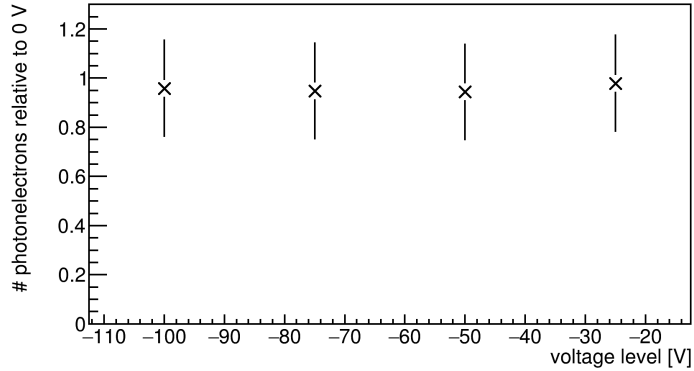


**Figure 9.** Average light yield detected per unit length of muon tracks as a function of the SiPM floating voltage, relative to the average light yield with no floating voltage applied.

## 4 Summary

We propose a new concept of anode to read out a LArTPC, integrating charge and light sensors to perform native 3D reconstruction of an event, which can detect neutrino interactions from the MeV to GeV energy scale. In this paper, we present the first demonstration of such an anode plane using an integrated dual-pixel readout of light and charge pixels, based on a distributed arrangement of VUV SiPMs. We discuss the design of a small demonstrator, referred to as SoLAr Prototype-v1, which was operated in October 2022 at the University of Bern, and present first results. The detector prototype collected cosmic-ray muon tracks with unambiguous correlations between the light and charge information. We also study the charge readout per unit length to demonstrate that this detector has the potential to perform calorimetric measurements.

The results from this prototype provide valuable information for the design of future detectors using the integrated light-charge pixel concept. We are preparing next prototyping stages to characterize and optimize the capability of the SoLAr concept for LArTPCs to detect neutrino signals at the MeV-scale.

## Acknowledgements

This document was prepared by the SoLAr collaboration. The project has received funding from the European Union’s Horizon 2020 Research and Innovation programme under GA no 101004761, by the Italian Ministry for Research and University (MUR) under Grant Progetto Dipartimenti di Eccellenza 2023-2027, and by the Swiss National Science Foundation. It has also been supported by several of the collaborating institutions: CIEMAT; Lawrence Berkeley National Laboratory; University of Bern; University of Manchester; University of Milano-Bicocca and INFN Sezione di Milano-Bicocca.

## References

- [1] DUNE collaboration, B. Abi et al., *Deep Underground Neutrino Experiment (DUNE), Far Detector Technical Design Report, Volume I Introduction to DUNE*, *JINST* **15** (2020) T08008, [2002.02967].
- [2] HYPER-KAMIOKANDE collaboration, K. Abe et al., *Hyper-Kamiokande Design Report*, 1805.04163.
- [3] DUNE collaboration, B. Abi et al., *Long-baseline neutrino oscillation physics potential of the DUNE experiment*, *Eur. Phys. J. C* **80** (2020) 978, [2006.16043].
- [4] K. Kubodera and T.-S. Park, *The Solar HEP process*, *Ann. Rev. Nucl. Part. Sci.* **54** (2004) 19–37, [nucl-th/0402008].
- [5] SNO collaboration, B. Aharmim et al., *Search for hep solar neutrinos and the diffuse supernova neutrino background using all three phases of the Sudbury Neutrino Observatory*, *Phys. Rev. D* **102** (2020) 062006, [2007.08018].
- [6] F. Capozzi, S. W. Li, G. Zhu and J. F. Beacom, *DUNE as the Next-Generation Solar Neutrino Experiment*, *Phys. Rev. Lett.* **123** (2019) 131803, [1808.08232].
- [7] I. Gil Botella and A. Rubbia, *Decoupling supernova and neutrino oscillation physics with LAr TPC detectors*, *JCAP* **08** (2004) 001, [hep-ph/0404151].
- [8] G. L. Fogli, E. Lisi, A. Marrone and A. Palazzo, *Solar neutrinos: With a tribute to John. N. Bahcall*, in *3rd International Workshop on NO-VE: Neutrino Oscillations in Venice: 50 Years after the Neutrino Experimental Discovery*, pp. 69–80, 5, 2006. hep-ph/0605186.
- [9] DUNE collaboration, B. Abi et al., *Supernova neutrino burst detection with the Deep Underground Neutrino Experiment*, *Eur. Phys. J. C* **81** (2021) 423, [2008.06647].
- [10] S. Parsa et al., *SoLAr: Solar Neutrinos in Liquid Argon*, *Snowmass 2021* (2022) , [2203.07501].
- [11] DUNE collaboration, V. Hewes et al., *Deep Underground Neutrino Experiment (DUNE) Near Detector Conceptual Design Report*, *Instruments* **5** (2021) 31, [2103.13910].
- [12] DUNE collaboration, A. Abed Abud et al., *Snowmass Neutrino Frontier: DUNE Physics Summary*, 2203.06100.
- [13] DUNE collaboration, *DUNE Phase-II: Scientific Opportunities, Detector Concepts, Technological Solutions*, 2024.
- [14] D. A. Dwyer et al., *LArPix: Demonstration of low-power 3D pixelated charge readout for liquid argon time projection chambers*, *JINST* **13** (2018) P10007, [1808.02969].
- [15] COMSOL Multiphysics © v.6.2, COMSOL AB, Stockholm, Sweden. <https://www.comsol.com>.
- [16] H. Pernegger and M. Friedl, “ROOT reference guide: Convoluted Landau and Gaussian Fitting Function.” [https://root.cern/doc/master/langaus\\_8C.html](https://root.cern/doc/master/langaus_8C.html).
- [17] DUNE collaboration, A. Abed Abud et al., *Performance of a modular ton-scale pixel-readout liquid argon time projection chamber*, 2403.03212.